# CZTS THIN FILMS GROWN BY SULFURIZATION OF ELECTRODEPOSITED METALLIC PRECURSORS: THE EFFECT OF INCREASING TIN CONTENT OF THE METALLIC PRECURSORS ON THE STRUCTURE, MORPHOLOGY AND OPTICAL PROPERTIES OF THE THIN FILMS[†]

## E.A. Botchway, Francis Kofi Ampong, Isaac Nkrumah*, D.B. Puzer, Robert Kwame Nkum, Francis Boakye

*Department of Physics, Kwame Nkrumah University of Science and Technology, Kumasi, Ghana*
*Corresponding Author e-mail: inkrumah.sci@knust.edu.gh*

A study has been carried out to investigate the influence of the amount of Sn in the precursor solution, on some physical properties of CZTS films grown by sulfurization of electrodeposited metallic precursors. The growth of the CZTS samples was achieved by sequential electrodepositon of constituent metallic layers on ITO glass substrates using a 3-electrode electrochemical cell with graphite as a counter electrode and Ag/AgCl as the reference electrode. The Sn-content in the metallic precursor was varied by varying the deposition time of Sn. The stacked elemental layer was then soft annealed in Argon at 350 °C, and subsequently sulfurized at 550° C to grow the CZTS thin films. The structure, morphology and optical properties were investigated. X-ray diffraction studies revealed that, irrespective of the Sn content all the films were polycrystalline and exhibited the Kesterite CZTS structure with preferred orientation along the (112) plane. However, there was an increase in the amount of peaks indexed to the undesirable secondary phases, as the Sn content in metallic precursor was increased. Optical absorption measurements revealed the existence of a direct transition with band gap values decreasing from 1.74 eV to 1.25 eV with increasing amounts of Sn. The lower value for the band gap was attributed to the presence of secondary phases formed in addition to the CZTS film. Morphology of the sulfurized films showed a compact and rocky texture with good coverage across the entire substrate. However, CZTS films with a higher Sn content appeared to have a molten metallic surface with deep cracks which could have adverse effects on the electrical properties of the film. EDAX analysis showed all the films were consistent with the formation of CZTS. It is evident from all the characterization techniques that increasing the Sn content of the stacked metallic precursors beyond stoichiometric amounts had an adverse effect on the structural and optical properties of CZTS films grown by this technique.

**Keywords:** *CZTS thin films; electrodeposition, sulfurization; characterization*
**PACS:** 81.15.-z, 68.55.-a, 78.20.-e

## INTRODUCTION

New types of thin film solar cells made from earth-abundant, and environmentally benign materials with adequate physical properties such as energy band-gap, large absorption coefficient and p-type conductivity are needed in order to replace the current technology based on $CuInGaSe_2$ and CdTe absorber materials, which contain scarce and toxic elements. One material which has been largely explored because of its suitability as a solar cell absorber layer, is $Cu_2ZnSnS_4$ (CZTS). This material is one of the ideal candidates for the production of thin film solar cells at large scale due to the natural abundance of all the constituent elements [1, 2]. CZTS has a direct band gap of ~ 1.5 eV, a large absorption coefficient greater than $10^{-4}$ $cm^{-1}$ and low thermal conductivity [3]. It is a p-type semiconductor that matches well with the solar spectrum, and it has achieved a benchmark power conversion efficiency of more than 10% [4].

The need for synthesis of new materials for industrial applications has resulted in a tremendous increase of innovative thin film processing technologies [5]. CZTS thin films, have been synthesized by various techniques. These include: Rf sputtering, co-evaporation, hybrid sputtering, photochemical deposition, sulfurization of electrochemically deposited metallic precursors among others. However, electrodeposition has emerged as one of the versatile and cost-effective growth technique of metal, metalloid and semiconductor materials [6, 7]. Production of thin film semiconductors for photovoltaics using electrodeposition gives several advantages when compared to other methods of deposition: the technique is simple and is carried out using low cost apparatus, low operating temperature, and economical due to its low material wastage. Depending on the electrical parameters such as electrode potential and current density, the thin film thickness can be controlled in a precise manner. Electrodeposition method has been used for the preparation of thin and thick films of metals, magnetic materials, super capacitive materials and chalcogenides [8].

Available literature indicates that the production of CZTS thin films by a two-step process involving the sulfurization of electrochemically deposited metallic precursors, has been reported as producing some of the best CZTS thin films. This has prompted several research groups to investigate various aspects needed to improve this synthesis route such as; techniques to address the volatility of certain elements, especially Sn at elevated temperatures [9, 10]. Others like Borate et al. [11], have examined the effect of deposition potential on the composition and morphology of CZTS thin films, whilst Mahjoubi et al. [12] reported on the influence of the concentration of Cu in the precursor solution, on some

---

properties of the films. Payno et al. [13] published an article on the effect of sulfurization temperature on a CZTS solar cell. These investigations are needed to determine the right synthesis conditions needed for optimum device performance. In spite of all these efforts, Sn loss always occurs during the sulfurization process [14], therefore, fabrication of high quality CZTS thin films is of great challenge [15]. Larramona et al. [16], have confirmed that controlling Sn losses in the annealing environment could improve the efficiency of CZTS solar cells, significantly and reproducibly.

In this paper, we report on the effect of increasing the amount of Sn in the precursor solution, on the structure, morphology and optical band gap of CZTS films grown by sulfurization of electrochemically deposited metallic precursors. The choice of electrode materials, was based on Botchway et al. [17]. To the best of our knowledge, such an investigation has rarely been sighted in literature.

## METHODOLOGY
### Substrate preparation

Indium-doped tin oxide (ITO) glass substrates were used. The substrates were cleaned by first dipping them into a beaker containing acetone and placed on an ultrasonic cleaner for a few minutes and then rinsed with deionized water. They were then transferred into a beaker containing ethanol and sonicated for another 5 minutes. After rinsing again with deionized water, the substrates were kept in dilute nitric acid for 5 minutes and rinsed with copious amounts of de-ionized water. After the cleaning process was complete, the substrates were left to dry in a desiccator

### Preparation of the electrolyte solutions

Copper electrolyte was prepared by mixing together aqueous solutions of 0.24 M $CuSO_4.5H_2O$ (source of $Cu^{2+}$ ions) and 1.36 M $C_6H_5Na_3O_7.2H_2O$ (complexant) in a 100 ml beaker. The pH of resulting solution was adjusted to 3.00 by the dropwise addition of 1.00 M $C_4H_6O_6$ (tartaric acid). An acidic medium was used because $Cu^{2+}$ ions are thermodynamically more stable in acidic electrolytes than in an alkaline one [18].

The tin electrolyte was prepared by mixing together aqueous solutions of 0.55 M of $SnCl_2.2H_2O$ (source of Sn (II) ions) and 1.00 M $C_6H_{14}O_6$ in a 100 ml beaker. Sorbitol ($C_6H_{14}O_6$) serves as a complexing agent and improves stability of Sn (II) and also adhesion of Sn [19]. The pH of the resulting solution was adjusted to 12.16 by adding a few drops of 2.25 M NaOH. An alkaline Sn electrolyte was chosen, because for the stacking sequence adopted for the deposition, copper was to be deposited first followed by Sn, an acid Sn electrolyte will dissolve the Cu layer already deposited on the substrate [20]. Secondly NaOH also serves to stabilize Sn (II) and prevent it from oxidizing to Sn (IV) which forms colloids and precipitate [21].

Zinc electrolyte was prepared from an aqueous solution of 0.10 M of $ZnSO_4.7H_2O$ (source of $Zn^{2+}$ ions), pH was adjusted to 6.26 by adding a few drops of 35 % ammonia solution. Aqueous ammonia, acts as a buffer to prevent large changes in pH at the electrode surface. Electrolyte volumes of ~75 ml ensured that concentration of metal cations was virtually constant during electrodeposition. All chemicals used were of Analytical reagent grade.

### Electrodeposition of the metallic precursors

The deposition of the metallic precursors was carried out sequentially from different batch solutions in the order, Cu/Sn/Zn. This technique was used to deposit the metallic precursors because it is easier to control the composition of the CZTS film and secondly, the highest efficiency CZTS solar cells have been fabricated via the SEL approach [22].

Prior to electrodeposition of the metal precursors, an ER 466 EDAQ computerized Potentiostat system was used to perform cyclic voltammetry (CV) on the individual electrolyte solutions to determine deposition potentials for the metallic elements of interest. Electrodeposition of each metal layer was carried out at these predetermined potentials.

High quality films of Cu, Sn and Zn were then deposited at -0.6 V, -1.10 V and -1.30 vs Ag/AgCl respectively. All depositions were at room temperature (30 ± 2 °C).

The thickness of the stacked elemental layers was well controlled by controlling the deposition time to achieve the desired composition. Each deposited film was tested for adhesion by placing it in a steady flow of distilled water before the subsequent deposition. To produce films with the required stoichiometry, the electrodeposition time reached for Cu, Sn and Zn was 10, 10 and 15 min. These deposition times were employed to achieve an optimum component atom ratio of Cu:Sn:Zn = 2:1:1. Which is the right stoichiometric ratio for the CZTS films.

To vary the Sn-content in the metallic precursors, different samples (metallic stacks) were prepared with the deposition time of Sn controlled for 1, 5, 10 and 15 minutes respectively, keeping all other deposition parameters constant.

Table 1 shows how the thickness of the Sn layer varied with deposition time. The thicknesses were measured by the gravimetric technique explained in Mondal et al. [23].

**Table 1.** Variation of the thickness of the Sn layer with deposition time

| Time/minutes | 1 | 5 | 10 | 15 |
|---|---|---|---|---|
| thickness/μm | 1.243626 | 1.4020705 | 1.559188 | 1.863976 |

Table 1 confirms an increase in Sn content with deposition time. It should be mentioned that these figures only reflect the Sn content in the metallic precursors and not in the CZTS film formed after sulfurization. As mentioned earlier, Sn loss always occurs during the sulfurization process [14].

### Post Deposition Treatment

The stacked metallic precursor were first soft annealed in argon at a temperature of $\sim 350$ °C to improve intermixing of the elements Cu-Sn-Zn and subsequently sulfurized at 550 °C to obtain the CZTS thin films. The techniques employed for the soft annealing and sulfurization process are as described by Botchway et al [17] and Puzer et al. [24].

### Thin Film Characterization

All XRD data were obtained using a PANalytical Empyrean Series 2 powder X-ray diffractometer with a Cu-kα radiation (1.5406 Å) in the 2θ range 10 to 90. The machine was operated at 40 mA and 45 kV for phase analysis using the Bragg-Brentano geometry. Total analysis time per samples was around 35 minutes for a 2θ scan step of 0.06°. XRD data treatment and analysis were carried out using high score plus software packages. A Cecil CE7500 series double beam UV-Visible spectrometer operating in the wavelength range of 190 nm to 1100 nm, a step height of 0.3 nm and a scan rate of 5 nm per second was used for optical absorbance measurements on thin films. Scanning electron microscopy (SEM) images and energy dispersive X-ray (EDX) analyses were obtained using a Phenom instrument with nominal electron beam voltages of 15 kV respectively.

## RESULTS AND DISCUSSION
### X-Ray Diffraction Studies

The X-ray diffraction (XRD) patterns for various stages of the synthesis process, of the CZTS films deposited with the right stoichiometric ratios, are shown in Figure 1.
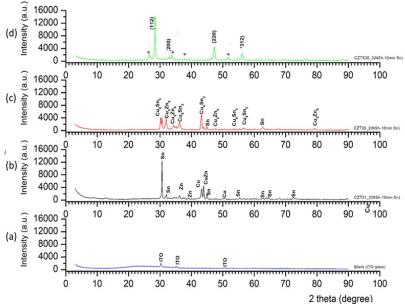


**Figure 1.** XRD pattern of (a) ITO glass substrate (b) as-deposited elemental stacks (c) metallic precursors, soft annealed at 350°C in Argon and (d) CZTS films formed after sulfurizing the metallic precursors at 550°C

Figure 1 shows the diffraction patterns of the film at various stages of the synthesis process for growing CZTS films with the right stoichiometry. The deposition time was 10 minutes for Cu and Sn, and 15 minutes for Zn.

Figure 1(b) is the diffractogram of the as-deposited stacked metallic layers. The assignments of peaks confirm the presence of Cu, Sn, and Zn. The peak at 2θ position 44 was indexed to the binary compound $Cu_1Zn_1$.

Figure 1 (c) shows the diffractogram after soft annealing the metallic precursors in Argon at 350 °C. Indexing the peaks revealed that at this stage the film was composed of the following binary compounds: $Cu_5Zn_8$ and $Cu_6Sn_5$. A few low intensity peaks were assigned to Sn.

The diffractogram in Figure 1 (d) confirms the formation of the kesterite CZTS phase after sulphurizing the films at 550°C. The prominent peaks observed at 2θ position 28.4446°, 32.8765°, 47.3409° and 56.1703° were indexed to reflections from the (112), (200), (220) and (312) planes of the kesterite structure $Cu_2ZnSnS_4$. A few impurity peaks labelled with asterisks are also observed in the diffractogram of Figure 1d. These impurity peaks are referenced to $Cu_2S_1$ (PDF card # 98-002-0560), $Cu_2SnS_3$ (PDF card # 00-027-0198) and $SnS_2$.

Figure 2 compares the diffraction patterns of the Kesterite CZTS thin films obtained after sulfurizing the electrodeposited metallic precursors containing different amounts of Sn. In other the precursor solutions used for these films do not contain right stoichiometric amount of Sn.

From Figure 2, it is evident that as the deposition time of Sn, and thus the amount of Sn in the metallic precursor is increased, the resulting CZTS film formed after sulfurization has an increasing number of peaks associated with impurities. These impurities, called secondary phases are due to the presence of compounds such as $Cu_2S_1$, $Cu_2SnS_3$ and $SnS_2$ which are formed in addition to the CZTS compound.
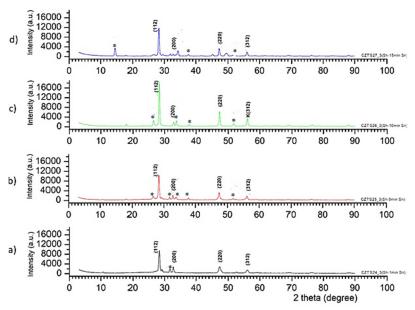
**Figure 2.** XRD patterns of the Kesterite CZTS obtained after sulfurizing the metallic precursors for the different deposition times of Sn: (a) 1 minute (b) 5 minutes (c) 10 minutes (d) 15 minutes

The formation of secondary phases, is due to the volatile nature of certain key elements such as Zn, and SnS under certain reaction conditions [9]. The loss of Sn through desorption of SnS from CZTS during annealing/sulfurization at elevated temperatures (400°C) is well documented by many researchers [10]. These have an adverse effect on some electrical, optical, and structural properties. From figure 2a, the precursor solution with the 1-minute deposition time for Sn, had the least number of impurities/secondary phases. A publication by Scragg *et al.* [25], offers some explanation for this observation. According to the authors, a stoichiometry of $Zn/Sn = 1$ produces the best quality films. In this work, the conditions used, produced a very thin layer of Zn, thus, the one-minute deposition time of Sn might just be enough to create a stoichiometry close to $Zn/Sn = 1$, thus producing the best films. However, this observation would have to be probed further. It is also important to note that, most of the impurities/secondary phases such as; cubic $Cu_2SnS_3$ and cubic ZnS have peak positions which are very similar to that of CZTS, due to similar crystal structure [21]. This makes it difficult to distinguish CZTS from these secondary phases in a diffractogram. However, some of the other secondary phases such as; $Cu_2S$ and SnS can be identified due to the peak positions which are entirely different from CZTS.

### Scanning electron microscopy

Figures 3 to 6 show the SEM images of the CZTS thin films grown at different deposition times of Sn. Figure 3 shows a non-uniform particle size with clearly defined large grains, formed from aggregation of small particles, spread non-uniformly among smaller grains on the surface of the substrate. The morphology is compact without any clear voids.

Figure 4 shows an increase in surface roughness with a larger number of grains with well-defined edges and shapes. This also shows a compact morphology without any clear voids.
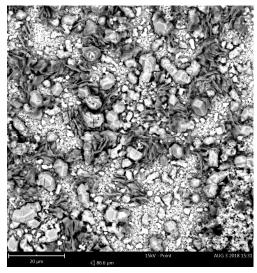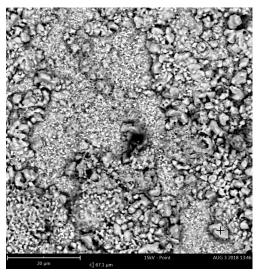


**Figure 3.** SEM image of CZTS thin film
(deposition time of Sn is 1 minute)



**Figure 4.** SEM image of CZTS thin film
(deposition time of Sn is 5 minute)

The film in Figure 5, appears compact with a relatively smoother texture and good coverage across the entire area of the substrate. Some areas look like a molten matrix composed of smaller grains. In Figure.6, the grains are no longer clearly defined and distinct. Instead, the surface appears to be disfigured with large sheets of a molten matrix which appears to have several cracks and voids. This type of morphology is not favorable for photovoltaic applications.
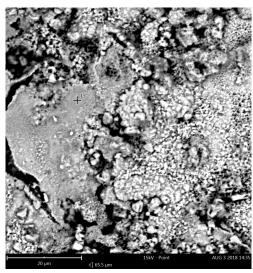


**Figure 5.** SEM image of CZTS thin film (deposition time of Sn is 10 minute)



**Figure 6.** SEM image of CZTS thin film (deposition time of Sn is 15 minute)

## ENERGY DISPERSIVE X-RAY SPECTROSCOPY (EDAX)

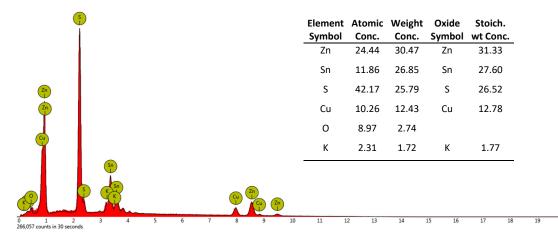The EDAX spectra of some of the CZTS films are shown in Figures 7 and 8.



| Element Symbol | Atomic Conc. | Weight Conc. | Oxide Symbol | Stoich. wt Conc. |
|---|---|---|---|---|
| Zn | 24.44 | 30.47 | Zn | 31.33 |
| Sn | 11.86 | 26.85 | Sn | 27.60 |
| S | 42.17 | 25.79 | S | 26.52 |
| Cu | 10.26 | 12.43 | Cu | 12.78 |
| O | 8.97 | 2.74 | | |
| K | 2.31 | 1.72 | K | 1.77 |

266,057 counts in 30 seconds

**Figure 7.** EDX spectrum of the CZTS thin film shown in Figure 3



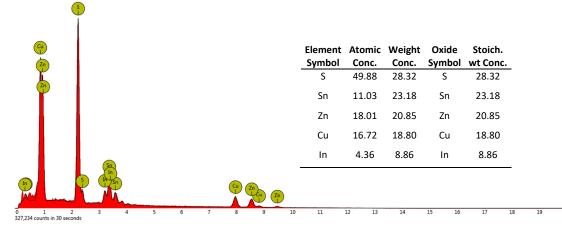| Element Symbol | Atomic Conc. | Weight Conc. | Oxide Symbol | Stoich. wt Conc. |
|---|---|---|---|---|
| S | 49.88 | 28.32 | S | 28.32 |
| Sn | 11.03 | 23.18 | Sn | 23.18 |
| Zn | 18.01 | 20.85 | Zn | 20.85 |
| Cu | 16.72 | 18.80 | Cu | 18.80 |
| In | 4.36 | 8.86 | In | 8.86 |

327,234 counts in 30 seconds

**Figure 8.** EDX spectrum of the CZTS thin film shown in Figure 5

Figures 7 and 8 show the EDAX spectrum and elemental composition of some of the CZTS thin films. The EDAX analyses of the films are consistent with the formation of CZTS. Other elements such as O, K, and In may emanate from the substrate.

### Results of the optical absorption spectroscopy

The optical properties, like other properties of thin films, show profound sensitivity on the film microstructure. Any changes in the electronic structure of the material would be reflected in its optical behavior [26].
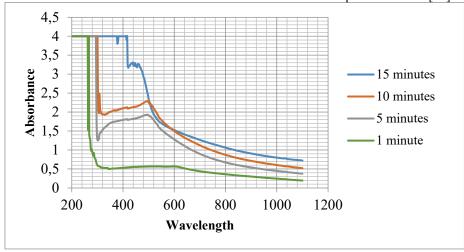


**Figure 9.** A plot of absorbance against wavelength for CZTS films prepared at different deposition times of Sn.

Figure 9 shows the absorbance for the CZTS samples prepared at different deposition times of Sn in the precursor solution. It can be observed that the absorbance increases with increasing deposition times of Sn. This behavior could be attributed to the formation of photon absorption sites caused by the presence of secondary phases. This view is supported by results from the XRD analysis which shows an increase in impurity peaks/secondary phases with increasing deposition time of Sn.

### Determination of the optical band gap

The energy band gap and type of electron transition were determined by the Stern relationship [27, 28] which is given by the expression:

$$A = \frac{[k(h\nu - E_g)]^{n/2}}{h\nu}$$

where A is the absorbance, $E_g$ is the band gap, $\nu$ is the frequency, h is the Planck's constant, k is a constant. The value of n is 1 and 4 for the direct transition and indirect transition respectively.

CuS, ZnS and SnS are all direct band gap materials. Thus, we assume that their mixed compositions would also have a direct band gap and hence, n is taken as 1. The energy band gap is obtained by plotting a line of best fit to the linear portion of the graph and extrapolating it to the point where it intersects the $h\nu$ axis as shown in Figures 10 and 11.
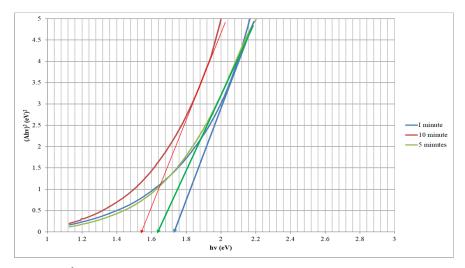


**Figure 10.** Plot of $(Ah\nu)^2$ versus $h\nu$ for the CZTS films grown with a 1, 5 and 10-minute deposition time of Sn

From Figures 10 and 11, the estimated band gaps are 1.74 eV, 1.62 eV, 1.54 eV and 1.25 eV for the 1, 5, 10- and 15-minutes deposition time of Sn. These values compare well with the values obtained by Khammar et al. [29]. The lower values for the higher deposition times may be attributed to the presence of secondary phases such as $Cu_2S$, $SnS$, and $Cu_2SnS_3$ formed in addition to the CZTS film.
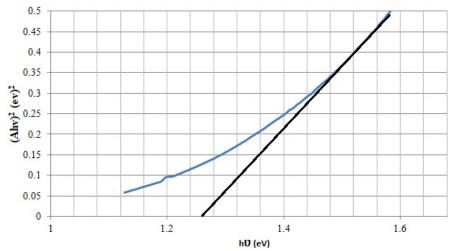


**Figure 11.** Plot of $(Ahv)^2$ versus $hv$ for the CZTS films grown with a 15-minute deposition time of Sn

### CONCLUSION

The effect of increasing Sn-content on the structure and optical properties of CZTS films grown by sulfurization of electrodeposited metallic precursors, has been studied. X-ray diffraction measurements showed that the kesterite CZTS structure was not altered by increasing the Sn content in the metallic precursor, however, there was an increase in the number of impurity peaks which were indexed to the presence of compounds such as $Cu_2S_1$, $Cu_2SnS_3$ and $SnS_2$ which are formed in addition to the CZTS compound. Optical absorption measurements revealed an increase in absorbance due to the presence of secondary phases. All the films showed direct transition with an estimated band gap which decreased from 1.74 eV to 1.25 eV with increasing Sn content. The lower value for the band gap was attributed to the presence of secondary phases formed in addition to the CZTS film. Morphology of the sulfurized films showed a compact and rocky texture with good coverage across the entire substrate. However, films with a higher Sn content appeared to have a molten metallic surface with deep cracks after sulfurization, making it unfavorable for photovoltaic applications. EDAX analysis confirmed the formation of CZTS. In conclusion, results of all the characterization techniques indicate that although the synthesis technique used in this work produced kesterite CZTS films with good crystallinity and favorable optical properties, increasing the Sn content of the metallic precursors beyond stoichiometric amounts had an adverse effect on all the physical properties investigated.

### ORCID IDs
**Isaac Nkrumah**, https://orcid.org/0000-0003-4030-7931; **Francis Kofi Ampong**, https://orcid.org/0000-0003-3562-8183
**Robert Kwame Nkum**, https://orcid.org/0000-0003-0404-760X

### REFERENCES
[1]  S.D. Sharma, K. Bayikadi, S. Raman, and S. Neeleshwar, Nanotechnology, **31**, (36), 365402 (2020). https://doi.org/10.1088/1361-6528/ab9393
[2]  S. Prabhu, S.K. Pandey, and S. Chakrabarti, International Journal of Energy Research, **46**(11), 15300 (2022). https://doi.org/10.1002/er.8232
[3]  K. Diwate, K. Mohite, M. Shinde, S. Rondiya, A. Pawbake, A. Date, H. Pathan, and S. Jadkar, Energy Procedia, **110**, 180 (2017). https://doi.org/10.1016/j.egypro.2017.03.125
[4]  D.B. Mitzi, O. Gunawan, T.K. Todorov, K. Wang, and S. Guha, Solar Energy Materials and Solar Cells, **95**(6), 1421 (2011). https://doi.org/10.1016/j.solmat.2010.11.028
[5]  S. Giraldo, Z. Jehl, M. Placidi, V. Izquierdo-Roca, A. Pérez-Rodríguez, and E. Saucedo, Advanced Materials, **32**, 1806692 (2019). https://doi.org/10.1002/adma.201806692
[6]  C. Gougaud, D. Rai, S. Delbos, E. Chassaing, and D. Lincot, Journal of The Electrochemical Society, **160**(10), 485 (2013). https://doi.org/10.1149/2.105310jes
[7]  I. Nkrumah, F.K. Ampong, A. Britwum, M. Paal, B. Kwakye-Awuah, R.K. Nkum, and F. Boakye, Chalcogenide Letters, **20**(3), 205 (2023). https://doi.org/10.15251/CL.2023.203.205
[8]  S. Thanikaikarasan, T. Mahalingam, T. Ahamad, S. M. Alshehr, Journal of Saudi Chemical Society, **24**, 955 (2020). https://doi.org/10.1016/j.jscs.2020.10.003

[9]    N. Jahan, R. Matin, M.S. Bashar, M. Sultana, M. Rahaman, M.A. Gafur, M.A. Hakim, et al., Am. Int. J. Res. Sci. Technol. Eng. Math, **1**, 69 (2016). http://iasir.net/AIJRSTEMpapers/AIJRSTEM16-141.pdf

[10]   A. Weber, R. Mainz, and H.W. Schock, Journal of Applied Physics, **107**(1), 013516 (2010). https://doi.org/10.1063/1.3273495

[11]   H. Borate, A. Bhorde, A. Waghmare, S. Nair, P. Subhash, A. Punde, P. Shinde, et al., ES Materials & Manufacturing, **11**, 30 (2020). http://dx.doi.org/10.30919/esmm5f934

[12]   S. Mahjoubi, N. Bitri, M. Abaab, and I. Ly, Materials Letters, **216**, 154 (2018). https://doi.org/10.1016/j.matlet.2018.01.004

[13]   D. Payno, S. Kazim, M. Salado, and S. Ahmad, Solar Energy, **224**, 1136 (2021). https://doi.org/10.1016/j.solener.2021.06.038

[14]   H. Zhang, M. Xie, S. Zhang, and Y. Xiang, Journal of Alloys and Compounds, **602**, 199 (2014). http://dx.doi.org/10.1016/j.jallcom.2014.03.014

[15]   S. Siebentritt, and S. Schorr, Progress in Photovoltaics: Research and Applications, **20**(5), 512 (2012). https://doi.org/10.1002/pip.2156

[16]   G. Larramona, S. Levcenko, S. Bourdais, A. Jacob, C. Choné, B. Delatouche, C. Moisan, et al., Advanced Energy Materials, **5**(24), 1501404 (2015). https://doi.org/10.1002/aenm.201501404

[17]   E.A. Botchway, F.K. Ampong, I. Nkrumah, R.K. Nkum, and F. Boakye, Open Journal of Applied Sciences, **9**(9), 725 (2019). https://doi.org/10.4236/ojapps.2019.99059

[18]   J.J. Scragg, T. Ericson, T. Kubart, M. Edoff, and C. Platzer-Bjorkman, Chemistry of Materials, **23**(20), 4625 (2011). https://doi.org/10.1021/cm202379s

[19]   S. Chen, J. Tao, H. Tao, Y. Shen, L. Zhu, J. Jiang, X. Zeng, and T. Wang, Materials Technology, **30**(5), 306 (2015). https://doi.org/10.1179/1753555715Y.0000000007

[20]   X. He, H. Shen, J. Pi, C. Zhang, and Y. Hao, Journal of Materials Science: Materials in Electronics, **24**(11), 4578 (2013). https://doi.org/10.1007/s10854-013-1445-2

[21]   T. Hreid, Doctoral dissertation, Queensland University of Technology, 2016.

[22]   F. Jiang, S. Ikeda, Z. Tang, T. Minemoto, W. Septina, T. Harada, and M. Matsumura, Research and Applications, **23**(12), 1884 (2015). https://doi.org/10.1002/pip.2638

[23]   S. Mondal, S.R. Bhattacharyya, and P. Mitra, Bulletin of Materials Science, **36**, 223 (2013). https://doi.org/10.1007/s12034-013-0462-3

[24]   D.B. Puzer, I. Nkrumah, F.K. Ampong, M. Paal, E.A. Botchway, R.K. Nkum, F. Boakye, Chalcogenide Letters, **18**(8), 481 (2021). https://chalcogen.ro/481_PuzerDB.pdf

[25]   J.J. Scragg, P.J. Dale, L.M. Peter, G. Zoppi, and I. Forbes, Physica Status Solidi B, **245**(9), 1772 (2008). https://doi.org/10.1002/pssb.200879539

[26]   O.V. Goncharova, and V.F. Gremenok, Semiconductors, **43**, 96 (2009). https://doi.org/10.1134/S1063782609010199

[27]   M. Paal, I. Nkrumah, F.K. Ampong, D.U. Ngbiche, R.K. Nkum, and F. Boakye, Science Journal of University of Zakho, **8**(3), 97 (2020). https://doi.org/10.25271/sjuoz.2020.8.3.752

[28]   C.K. Bandoh, I. Nkrumah, F.K. Ampong, R.K. Nkum, and F. Boakye, Chalcogenide Letters, **18**(2), 81 (2021). https://chalcogen.ro/81_BandohCK.pdf

[29]   M. Khammar, F. Ynineb, S. Guitouni, Y. Bouznit, and N. Attaf, Applied Physics A, **126**(6), 398 (2020). https://doi.org/10.1007/s00339-020-03591-6

**ТОНКІ ПЛІВКИ CZTS, ВИРОЩЕНІ ШЛЯХОМ СУЛЬФУРИЗАЦІЇ ЕЛЕКТРООСАДЖЕНИХ МЕТАЛЕВИХ ПРЕКУРСОРІВ: ВПЛИВ ПІДВИЩЕННЯ ВМІСТУ ОЛОВА В МЕТАЛЕВИХ ПРЕКУРСОРАХ НА СТРУКТУРУ, МОРФОЛОГІЮ ТА ОПТИЧНІ ВЛАСТИВОСТІ ТОНКИХ ПЛІВОК**

**Є.А. Ботчвей, Френсіс Кофі Ампонг, Ісаак Нкрума, Д.Б. Пузер, Роберт Кваме Нкум, Френсіс Боак'є**
*Факультет фізики, Університет науки і технологій Кваме Нкрума, Кумасі, Гана*

Було проведено дослідження впливу кількості Sn у розчині прекурсора на деякі фізичні властивості плівок CZTS, вирощених шляхом сульфування електроосаджених металевих прекурсорів. Зростання зразків CZTS було досягнуто шляхом послідовного електроосадження складових металевих шарів на скляних підкладках ITO з використанням 3-електродної електрохімічної комірки з графітом як протиелектродом та Ag/AgCl як електродом порівняння. Вміст Sn в металевому прекурсорі змінювали шляхом зміни часу осадження Sn. Складений елементний шар потім м'яко відпалювали в аргоні при 350°C, а потім сульфірували при 550°C для вирощування тонких плівок CZTS. Досліджено структуру, морфологію та оптичні властивості. Дослідження рентгенівської дифракції показали, що незалежно від вмісту Sn усі плівки були полікристалічними та демонстрували структуру кестериту CZTS з переважною орієнтацією вздовж площини (112). Однак спостерігалося збільшення кількості піків, індексованих до небажаних вторинних фаз, оскільки вміст Sn у металевому попереднику був збільшений. Вимірювання оптичного поглинання показало наявність прямого переходу зі значеннями забороненої зони, що зменшуються від 1,74 eB до 1,25 eB зі збільшенням кількості Sn. Менше значення ширини забороненої зони пояснюється наявністю вторинних фаз, утворених на додаток до плівки CZTS. Морфологія сульфурованих плівок показала компактну та кам'янисту текстуру з хорошим покриттям по всій підкладці. Однак плівки CZTS з більш високим вмістом Sn мали розплавлену металеву поверхню з глибокими тріщинами, які могли мати негативний вплив на електричні властивості плівки. Аналіз EDAX показав, що всі плівки відповідають утворенню CZTS. З усіх методів визначення характеристик очевидно, що збільшення вмісту Sn у складених металевих прекурсорах понад стехіометричні кількості мало несприятливий вплив на структурні та оптичні властивості плівок CZTS, вирощених цією технікою.
**Ключові слова:** *тонкі плівки CZTS; електроосадження, сульфуризація; дослідження*